Atmospheric Pollution Research 10 (2019) 168–179

HOSTED BY

Contents lists available at ScienceDirect

Atmospheric Pollution Research

journal homepage: www.elsevier.com/locate/apr

# Spatial and temporal disaggregation of natural emissions in urban areas in Greece for the period 2010–2013 and future projections

Victoria Aleksandropoulou, Mihalis Lazaridis*

*Department of Environmental Engineering, Technical University of Crete, Polytechneioupolis 73100 Chania, Greece*

ARTICLE INFO

*Keywords:*
Emission inventory
BVOCs
Natural emissions
Windblown dust
Climate change scenarios

ABSTRACT

Emission inventories for particulate matter ($PM_{2.5}$ and $PM_{2.5-10}$) from natural sources were created for the Athens and Thessaloniki metropolitan areas and the greater area of Volos for the period 2010–2013. The inventories include primary windblown dust emissions from agricultural and vacant lands, primary sea salt particles emissions from the breaking of waves at the Sea Shore-surf zone and the bursting of bubbles from oceanic whitecaps - Open Ocean, and emissions of BVOCs (Biogenic Volatile Organic Compounds), precursor to PM. The objective of this work was to study the seasonal variation of natural PM emissions in the areas of interest and their spatial allocation. Weighting factors, specific to each pollutant, source and area, were calculated for the disaggregation of annual emissions to monthly and daily values and their allocation on high resolution grids. There was no significant seasonal variation observed in the natural PM emissions while BVOCs emissions were increased during the warm period due to the enhanced solar radiation and temperature. The results of the calculations were compared to values of the period 2000–2010 and it was found that natural BVOCs emissions during the period 2010–2013 were enhanced compared to 2000–2010 whereas natural PM emissions have lowered. Moreover, the analysis focused on the effects from possible future changes in land cover and environmental conditions to the temporal and spatial variation of natural emissions over the areas using specific scenarios.

## 1. Introduction

The air quality deterioration related to ambient particulate matter in urban areas is associated with human health problems as highlighted from a number of epidemiological studies (e.g. Katsouyanni et al., 2001; Pope et al., 1995, 2002). In addition, the quantification of gaseous precursors and particulate air pollutant emissions from natural sources is an important task in order to quantify their ambient concentrations and to determine the importance of the different sources (e.g. Winiwarter et al., 2009; Aleksandropoulou et al., 2011, 2015; Hodnebrog et al., 2012).

Emission inventories including spatiotemporally allocated emissions from natural sources in Greece were presented in a number of studies (e.g. Aleksandropoulou and Lazaridis, 2004; Aleksandropoulou et al., 2015; Symeonidis et al., 2008; Athanasopoulou et al., 2010). Emission inventories for Greece from natural sources were incorporated also in European studies (e.g for Biogenic Volatile Organic Compounds (BVOCs) Oderbolz et al., 2013; for windblown dust (WB) Korcz et al., 2009).

In this work a spatially and temporally resolved emission inventory was used to examine the temporal evolution of PM emissions in the metropolitan areas of Athens, Thessaloniki and Volos for the period 2010–2013 (Fig. 1). The inventory includes the emissions of $PM_{2.5}$ and $PM_{2.5-10}$ from natural sources i.e. emissions of windblown dust from agricultural and vacant lands and sea salt particles emissions from the breaking of waves at the Sea Shore-surf zone (SS_SS) and the bursting of bubbles from oceanic whitecaps - Open Ocean (SS_OO). In addition, the inventory includes gaseous emissions from natural sources, in particular biogenic gaseous pollutants (BVOCs) emissions from vegetation during photosynthesis, plant respiration and vaporization from stores within the plant tissue. These gaseous emissions have the potential to form secondary organic particles in the atmosphere through chemical reactions. The methodology for the spatial and temporal disaggregation of the emission inventory is described and the analysis then is focused on the seasonal/monthly variation of particulate matter and their precursor gases emissions from natural sources and their spatial distribution. The temporal and spatial evolution of natural emissions in the metropolitan areas of Athens, Thessaloniki and Volos during the period

Peer review under responsibility of Turkish National Committee for Air Pollution Research and Control.
* Corresponding author.
*E-mail address:* lazaridi@mred.tuc.gr (M. Lazaridis).

https://doi.org/10.1016/j.apr.2018.07.003
Received 16 February 2018; Received in revised form 15 July 2018; Accepted 16 July 2018
Available online 23 July 2018

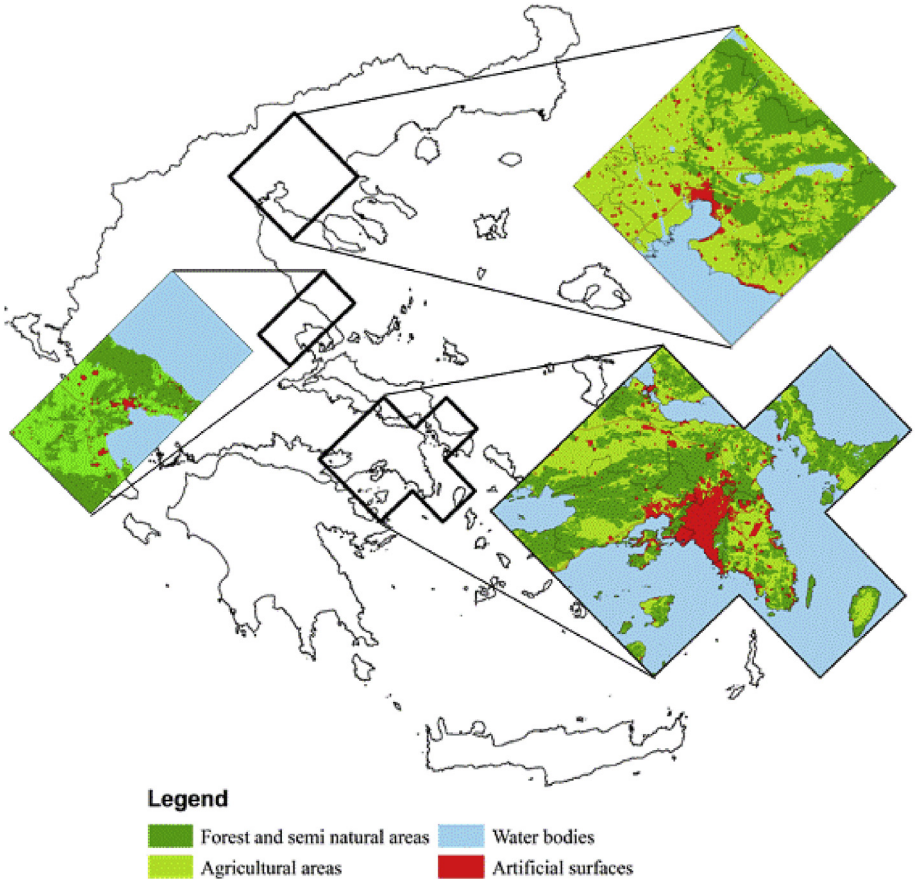


**Fig. 1.** Areas of interest and distribution of land cover (main classes; EEA CLC, 2009).

2010–2013 is examined and compared to the previous decade 2000–2010. Additionally, future temporal and spatial variations of natural emissions under different scenarios are presented.

## 2. Methodology

### *2.1. Input data and assumptions affecting the spatial and temporal variation of natural emissions*

A detailed description of the methodology used for evaluating the spatiotemporal distribution of natural emissions is presented by Aleksandropoulou et al. (2015). The temporal disaggregation is performed using calculated disintegration coefficients based on monthly and daily averages of meteorological conditions (monthly meteorology from FOODSEC Meteodata distribution page: action developed in the framework of the EC Food Security Thematic Programme; European Centre for Medium-Range Weather Forecast data ECMWF ERA INTERIM reanalysis model data; temporal analysis 10-days; spatial resolution 0.25°; daily meteorology from NCEP Reanalysis Derived data provided by the NOAA/OAR/ESRL PSD, Boulder, Colorado, USA, from their Web site at http://www.esrl.noaa.gov/psd/; Kalnay et al., 1996). The temporal resolution of meteorological data can affect the emission estimates especially on local scales as it has been previously shown by Ashworth et al. (2010) for global isoprene emission estimates.

The effects of using monthly averaged wind speed values instead of hourly data (particularly 3 h averages) in predicting the emissions of dust due to wind erosion and of sea salt particles in the calculations have been examined in Aleksandropoulou et al. (2013). It was found that although emission rates can differ substantially from the actual ones, the results as regards monthly emissions are acceptable since the error introduced by the above assumptions can be considered the same to that introduced by uncertainty in other parameters (i.e. the soil moisture content and texture, the surface roughness length, and constraining factors like the vegetation coverage and the presence of non-erodible elements). Moreover, the use of daily temperature data instead of monthly (NOAA/OAR/ESRL PSD data vs. ECMWF ERA INTERIM reanalysis model data) resulted in a difference in annual BVOCs emissions of −4.3% for AMA, −23% for TMA and 14% for GVA. With regards to the seasonal variation in BVOCs emissions the use of daily temperature values resulted in differences in the range of 4% and −58% for the warm and cold period in AMA, respectively while the corresponding values were −18% and −82% for TMA and 22% and −79% for GVA. Similar findings concerning isoprene emissions were derived by Pugh et al. (2013).

In the absence of other relevant data, it was assumed that the landcover remains unchanged throughout the period (Land Cover 2000 database of the European Commission programme to COoRdinate INformation on the Environment across Europe; EEA CLC 2000, v2009) (Aleksandropoulou et al., 2015). As with the annual natural emissions, the variation in monthly values due to changes in land cover caused from forest fires during the period 2000–2008 in the Athens Larger Urban Zone was examined in Aleksandropoulou et al. (2013).

### *2.2. Temporal disaggregation of emissions*

The variation in natural emissions depends on the meteorological conditions, the emission factors and changes in land use. Since land use data remained unchanged throughout the period, temporal disintegration coefficients depend solely on the meteorological conditions and the seasonal and hourly variation in emission factors.

The annual PM emissions are temporally disaggregated to hourly emissions using the function (Eq. (1)):

$$Em_{h,m,y,j,k} = E_{y,j,k}\frac{M_{y,m,j,k}}{12}D_{y,m,j,k}H_{y,m,j} \quad (1)$$

where $Em_{h,y,j,k}$ is the emission for hour h, month m, and year y, of pollutant j from source k; $E_{y,j,k}$ is the emission for year y, of pollutant j from source k; $M_{y,m,j,k}$, $D_{y,m,j,k}$ and $H_{y,m,j}$ are the monthly, daily and hourly disintegration coefficients for month m and year y, of pollutant j from source k; j = [$PM_{2.5}$; $PM_{2.5\text{-}10}$; BVOCs]; k = [SS_SS; SS_OO; WB; BVOCs]; y = (2000, 2010); m = (January, December); h = (1, 24).

The emission estimation methodology used in this study resulted in the calculation of emissions either in the form of hour/day averages (BVOCs) or as average emissions per second (SS, WB) for specific month and year which were then combined to produce annual emissions. Consequently, the monthly coefficients, $M_{y,m,j,k}$, for month m and year y, for pollutant j from source k were calculated based on the equation (Eq. (2)):

$$M_{y,m,j,k} = \frac{E_{y,j,k}}{12}E_{y,m,j,k} \quad (2)$$

where $E_{y,m,j,k}$ is the emission for year y, of pollutant j from source k and month m.

The emissions are equally distributed to each day of the month for SS while for WB and BVOCs emissions daily disintegration coefficients have been calculated based on the intermonth variation in daily wind speed and temperature values (data from NOA stations and NCEP Reanalysis Derived data provided by the NOAA/OAR/ESRL PSD, Boulder, Colorado, USA, from their Web site at http://www.esrl.noaa.gov/psd/; Kalnay et al., 1996). In particular, daily averages of BVOCs emissions have been calculated. Accordingly, the daily coefficients, $D_{y,m,j,k}$, for month m and year y, for pollutant j from source k in equation (1) equals to (Eq. (3)):

$$D_{y,m,j,k} = \begin{cases} \frac{1}{N_{m,y}}, & \textit{for SS emissions} \\ \frac{\overline{U_{d,m,y}}/\overline{U_{m,y}}}{N_{m,y}}, & \textit{for WB emissions} \\ \frac{E_{d,y,m,j,k}}{E_{y,m,j,k}}, & \textit{for BVOCs emissions} \end{cases} \quad (3)$$

where $N_{m,y}$ are the number of days in month m of year y, $\overline{U_{d,m,y}}$ is the day average of windspeed for day d of month m in year y, $\overline{U_{m,y}}$ is the monthly average of windspeed in year y, $E_{d,y,m,j,k}$ is the daily emission for month m of year y for pollutant j from source k and $E_{y,m,j,k}$ is the emission for year y, of pollutant j from source k and month m.

In addition, emissions can be equally distributed to each hour of the day, i.e. $H_{y,m,j}$ equals to (1/24). The latter applies only to PM emissions since BVOCs emissions depend also on light. The final temporal resolution of emissions is 1 h for $PM_{2.5}$ and $PM_{10\text{-}2.5}$ and 1 d for BVOCs.

Finally, the contribution of gaseous pollutants to aerosol formation was calculated for each source sector according to the methodology of De Leeuw (2002) and the application by Aleksandropoulou et al. (2015).

### 2.3. Future climate scenarios

Expected impacts from climate change to southern Europe relevant to natural emissions are decreased precipitation, increased temperature by 2.4 – 4 °C by 2071–2100 mostly during the summer, increased risk of forest fires, increase of growing season, reduction in summer soil moisture and increased aridity, contraction of forests, sea level rise and reduction in extent and duration of snow cover (EEA, 2012). Based on the above the following future scenarios were examined as regards BVOCs emissions:

(1) increase in artificial land by 2.7% with subsequent decrease in areas with natural, semi-natural and agricultural land cover (values according to changes in European land cover from 2000 to 2006; EEA, 2013) - the meteorological conditions are same as in 2013,
(2) all forests and semi-natural areas are burnt - unchanged meteorological conditions, and
(3) increase in temperature by 1–4 °C – land cover remains unchanged and same as for 2013.

In addition, the following scenarios were examined as regards soil dust emissions:

(1) intermediate case: periods with rain are considered inactive for dust emissions and all surfaces have unstable soil (unlimited erosion potential) – land use remains unchanged,
(2) worst case: no rain or ice is considered – dry conditions - – land use remains unchanged, and
(3) all forests and semi-natural areas are burnt-the meteorological conditions are same as in 2013 simulations for the worst case scenario.

The methodology for the calculation of biogenic emissions was based on the work of Aleksandropoulou et al. (2013, 2015).

Dust emissions (g/cm$^2$s) from wind erosion of agricultural and vacant lands were estimated as a function of landcover, soil texture, wind friction velocity and threshold friction velocity at the study. The sea salt emissions (in g/m$^2$s μm) by the breaking of waves at sea shore were estimated using the source function provided by De Leeuw et al. (2000) modified according to Zhang et al. (2005). The length of the coastline covering sea shore was calculated from relevant spatial data available from the Hellenic Ministry for the Environment, Energy and Climate Change (geodata.gov.gr) and the surf zone width was assumed equal to 50 m (mean surf-zone).

Hourly sea-salt particle emissions (particles/m$^2$s) from the sea surface ($PM_{10}$ disaggregated in eight size bins) were computed as a function of the wind speed and the size of particle which depends on the relative humidity (RH) of the atmospheric layer above the sea surface, according to Grini et al. (2002).

Finally, BVOCs emissions (in μg/month) were estimated using the modification of the methodology presented in the EMEP/CORINAIR

## 3. Results and discussion

### 3.1. Monthly variation of natural emissions

The monthly emissions of primary PM from natural sources in the three areas of interest during the period 2010–2013 and comparison with the period 2000–2010 are depicted in Figs. 2 and 3. Based on the assumptions made in the calculations it was found that the monthly variation of $PM_{2.5\text{-}10}$ windblown dust and sea-salt sea-shore emissions is the same as to $PM_{2.5}$ emissions but with higher values (therefore it is not presented in Fig. 3). In addition, it is observed that most of the emissions of natural PM occur during the cold period of the year at all areas. In particular, in AMA natural $PM_{2.5}$ and $PM_{2.5\text{-}10}$ emissions exhibit their lowest value in May ($PM_{2.5}$ SS_SS: 327.6 ± 27.9 t, SS_OO: 107.3 ± 37.6 t, WB: 17.4 ± 6.9 t; $PM_{2.5\text{-}10}$ SS_SS: 2552.2 ± 217.6 t, SS_OO: 601 ± 164 t, WB: 157 ± 61.8 t) and the highest in August ($PM_{2.5}$ SS_SS: 455.5 ± 55.6 t, SS_OO: 347.1 ± 124.3 t, WB: 77.7 ± 31.5 t; $PM_{2.5\text{-}10}$ SS_SS: 3548.7 ± 433.1 t, SS_OO: 1629 ± 528.7 t, WB: 699.4 ± 283.2 t) with a Warm/Cold period emission ratio equal to 0.91 for $PM_{2.5}$ and $PM_{2.5\text{-}10}$ SS_SS emissions, 0.96 for $PM_{2.5}$ and $PM_{2.5\text{-}10}$ WB emissions, 0.75 for $PM_{2.5}$ and 0.78 for $PM_{2.5\text{-}10}$ SS_OO emissions.

Likewise, in TMA natural $PM_{2.5}$ and $PM_{2.5\text{-}10}$ emissions exhibit their lowest value in November for sea-salt sea-shore particles and windblown dust ($PM_{2.5}$ SS_SS: 32.4 ± 2 t, WB: 2.6 ± 1.1 t; $PM_{2.5\text{-}10}$ SS_SS: 252.6 ± 15.8 t, WB: 23 ± 10 t) and in August for sea-salt particles from open ocean (SS_OO $PM_{2.5}$: 2.3 ± 0.3 t; $PM_{2.5\text{-}10}$: 32.4 ± 1.7 t) while the highest values are observed in January for sea-salt sea-shore particles (SS_SS $PM_{2.5}$: 37.4 ± 2.9 t, $PM_{2.5\text{-}10}$: 291.2 ± 22.9 t) and in

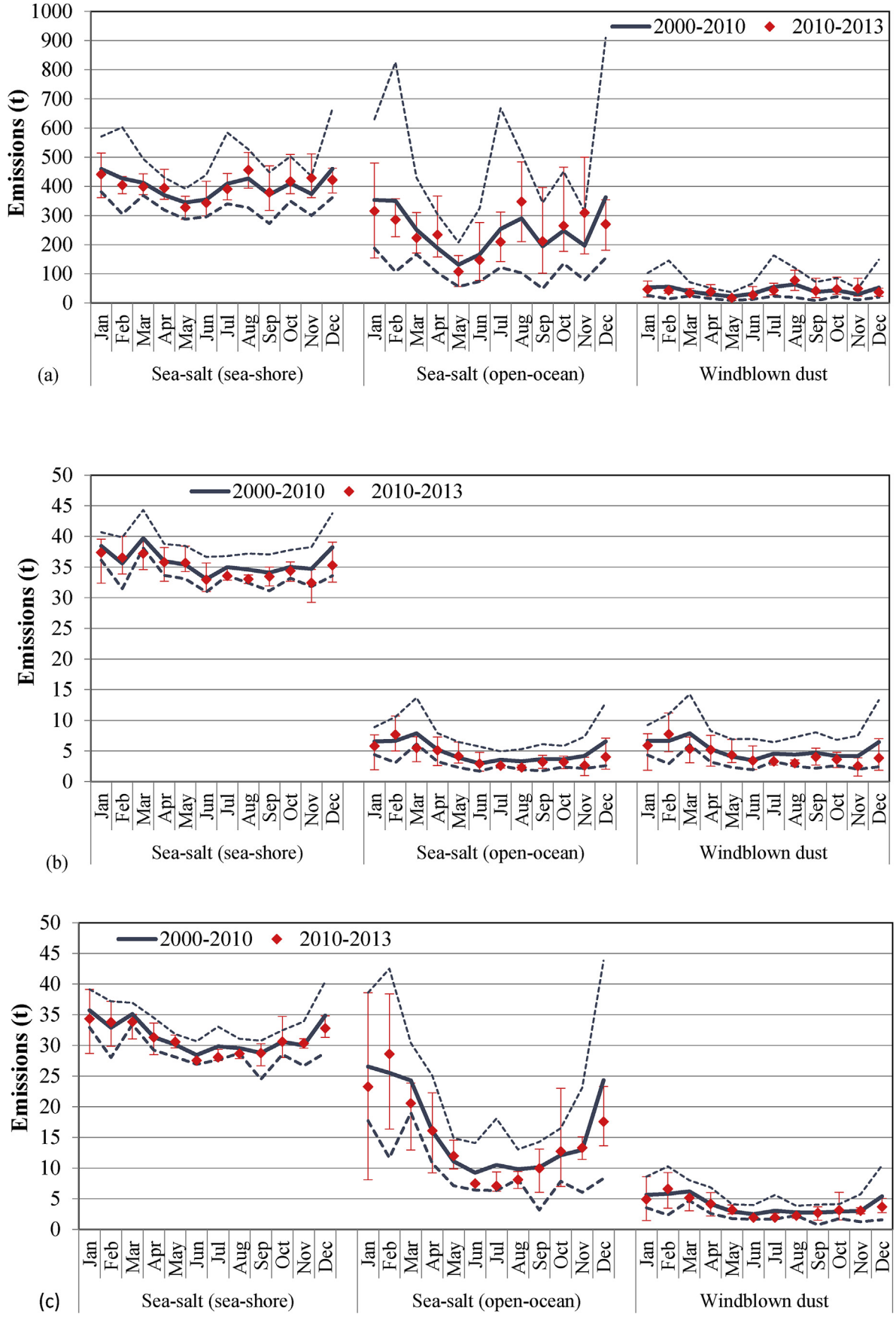


**Fig. 2.** Comparison between 2000-2010 and 2010–2013 of monthly variation of $PM_{2.5}$ emissions in (a) AMA, (b) TMA and (c) GVA. Average, minimum and maximum monthly emission values are depicted.

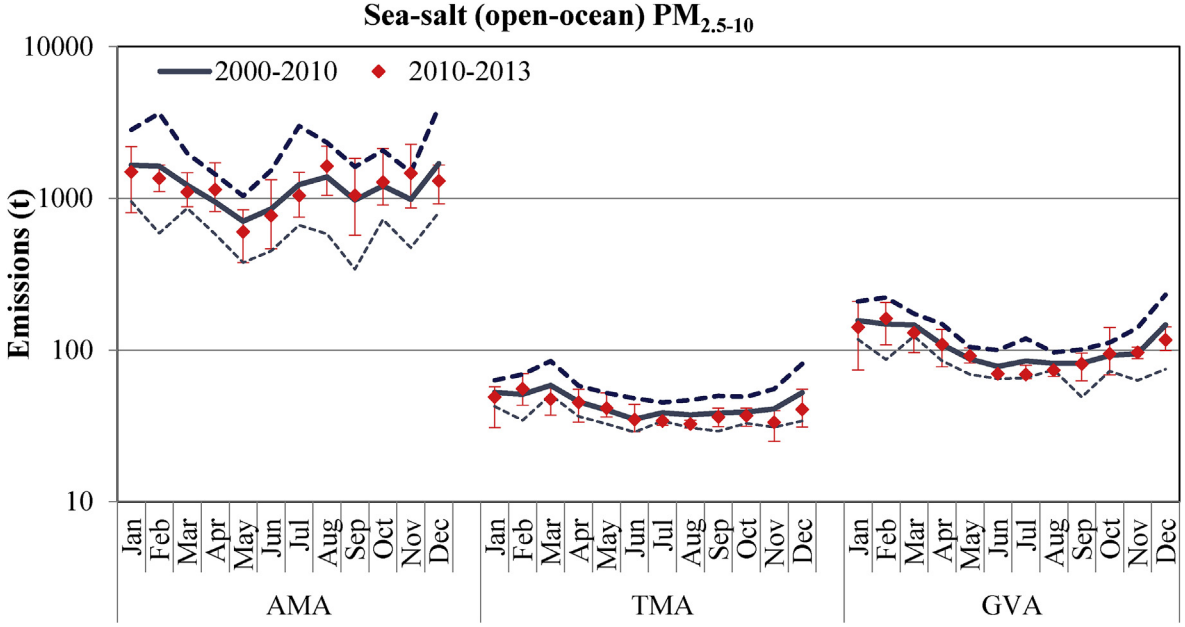


**Fig. 3.** Comparison between 2000-2010 and 2010–2013 of monthly variation of $PM_{2.5-10}$ emissions from open-ocean in AMA, TMA and GVA. Average, minimum and maximum monthly emission values are depicted.

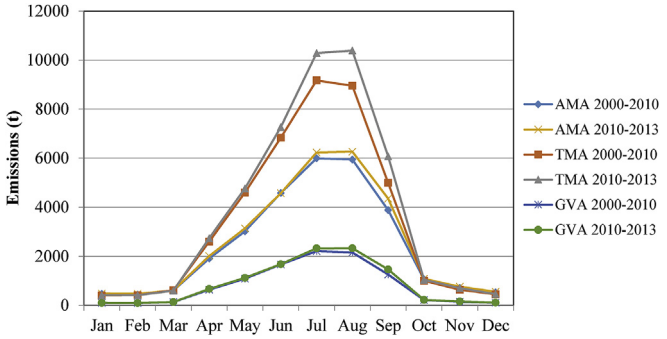


**Fig. 4.** Comparison between 2000-2010 and 2010–2013 of monthly variation of BVOCs emissions in AMA, TMA and GVA.

February for sea-salt particles from open ocean and windblown dust ($PM_{2.5}$ SS_OO: 7.7 ± 2.4 t, WB: 7.8 ± 2.7 t; $PM_{2.5-10}$ SS_OO: 55.4 ± 11.2 t, WB: 69.8 ± 24.2 t). The Warm/Cold period emission ratio equals to 0.96 for $PM_{2.5}$ and $PM_{2.5-10}$ SS_SS emissions, 0.8 for $PM_{2.5}$ and $PM_{2.5-10}$ WB emissions, 0.71 for $PM_{2.5}$ and 0.85 for $PM_{2.5-10}$ SS_OO emissions.

Finally in GVA natural $PM_{2.5}$ and $PM_{2.5-10}$ emissions exhibit their lowest value in June for sea-salt sea-shore particles (SS_SS $PM_{2.5}$: 27.5 ± 0.1 t, $PM_{2.5-10}$: 214.6 ± 0.6 t) and in July for sea-salt particles from open ocean and windblown dust ($PM_{2.5}$ SS_OO: 7.1 ± 1.3 t, WB: 1.9 ± 0.4 t; $PM_{2.5-10}$ SS_OO: 68.9 ± 6.1 t, WB: 17.4 ± 3.7 t) whereas the highest amount is emitted in January for sea-salt sea-shore particles (SS_SS $PM_{2.5}$: 34.3 ± 3.8 t, $PM_{2.5-10}$: 267.5 ± 29.4 t) and in February for sea-salt particles from open ocean and windblown dust ($PM_{2.5}$ SS_OO: 28.6 ± 7.9 t, WB: 6.6 ± 2.1 t; $PM_{2.5-10}$ SS_OO: 161.4 ± 34.9 t, WB: 59.4 ± 18.7 t). The Warm/Cold period emission ratio equal to 0.89 for $PM_{2.5}$ and $PM_{2.5-10}$ SS_SS emissions, 0.61 for $PM_{2.5}$ and $PM_{2.5-10}$ WB emissions, 0.52 for $PM_{2.5}$ and 0.67 for $PM_{2.5-10}$ SS_OO emissions.

Compared to the monthly variation of emissions in the period 2000–2010, it is observed that monthly emissions of the period 2010–2013 primarily have smaller variation (smaller variation in wind speed values). The monthly trend in sea salt sea-shore emissions is almost the same during both periods except for April, August, November and December in AMA for which the monthly contribution has changed 27.5%, 28.6%, 60% and −31.7%, respectively. The monthly trend in sea salt emissions from open ocean and windblown dust is different among the two periods (change of monthly contribution in absolute values WB: 42%–124% in AMA, 12%–156% in TMA, 16%–118% in GVA; $PM_{2.5}$ SS_OO: 36%–241% in AMA, 12%–144% in TMA, 18%–106% in GVA; $PM_{2.5-10}$ SS_OO: 31%–206% in AMA, 6%–74% in TMA, 17%–63% in GVA).

As previously mentioned, the monthly variation of natural PM emissions depends on the meteorological conditions. It is observed that sea salt emissions from the sea-shore do not exhibit significant seasonal variation. On the other hand, sea salt emissions from the open sea are more enhanced during the cold period of the year. This is attributed to the higher wind speeds during the cold period of the year. In AMA enhanced emissions of sea salt particles in summer can be attributed to the Etesians. As regards WB dust emissions, it was found that cold period emissions are enhanced and particularly in GVA are almost twice the warm period values.

The results of the calculations for monthly emissions of BVOCs during the period 2010–2013 are summarized in Fig. 4. It was found that BVOCs emissions are enhanced from April to September (warm season) due to the enhanced solar radiation and temperature. In addition, the maximum monthly emissions were observed in August at all areas (AMA: 6266 ± 428 t, TMA: 10388 ± 604 t, GVA: 2329 ± 175 t) and the minimum during February in AMA (469 ± 47 t) and GVA (97 ± 11 t) and during January in TMA (410 ± 38 t). During the warm period are emitted 86.9 ± 0.6%, 91.3 ± 0.4% and 91.9 ± 0.4% of annual BVOCs emissions in AMA, TMA and GVA, respectively. Compared to the previous period emissions remain relatively unchanged during the cold period and are slightly enhanced during the warm season. In addition, the maximum monthly emissions were observed in July during 2000–2010 whereas in the period 2010–2013 during August.

Aleksandropoulou et al. (2015) showed that the contribution from natural sources to $PM_{10}$ emissions was significant for the period 2000–2010 (~79% for AMA; ~46% for TMA). Similar contribution is expected for the period 2010–2013 since no considerable changes were observed in the meteorological conditions. However, the economic crisis in Greece after 2009 may change the picture due to reduction in vehicular traffic and industrial production and an increase of wood

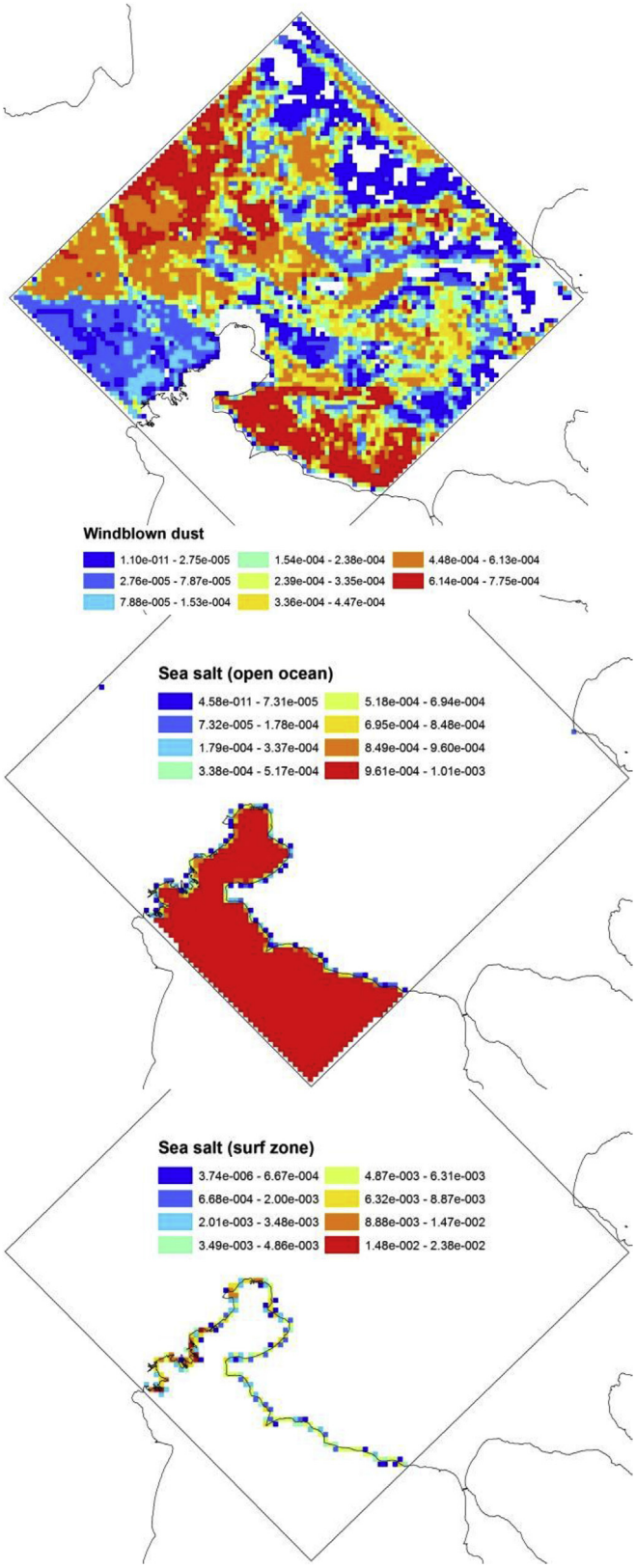


**Fig. 5.** Spatial distribution coefficients for $PM_{2.5}$ and $PM_{2.5\text{-}10}$ emissions of sea salt (open-ocean), sea salt (surf zone) and windblown dust for AMA and TMA.

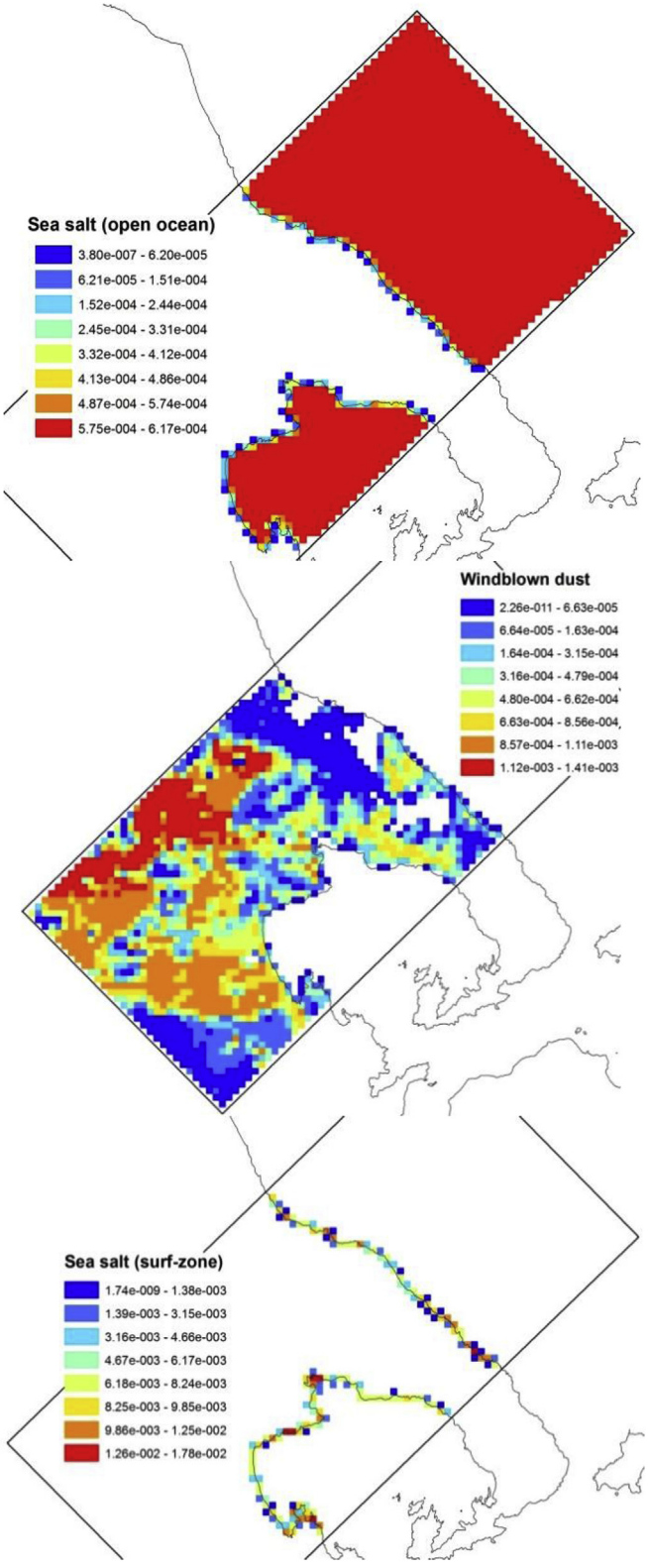


**Fig. 6.** Spatial distribution coefficients for $PM_{2.5}$ and $PM_{2.5\text{-}10}$ emissions of sea salt (open-ocean), sea salt (surf zone) and windblown dust for GVA.

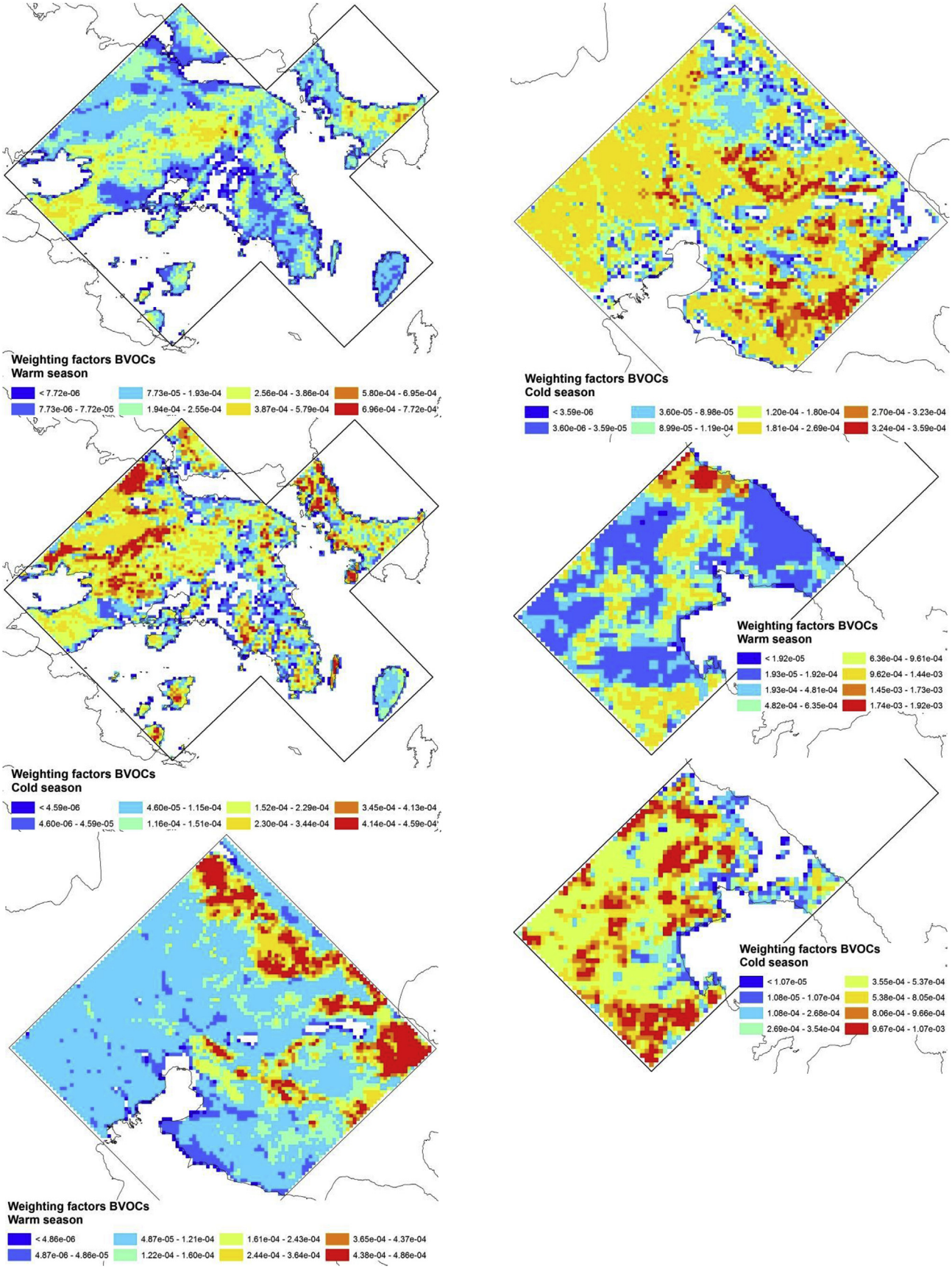


**Fig. 7.** Comparison between warm and cold period spatial weighting factors for BVOCs emissions in AMA, TMA and GVA. The values in the legend correspond to the 1%, 10%, 25%, 33%, 50%, 75%, 90% and 100% percentile of weighting factor values for each period.

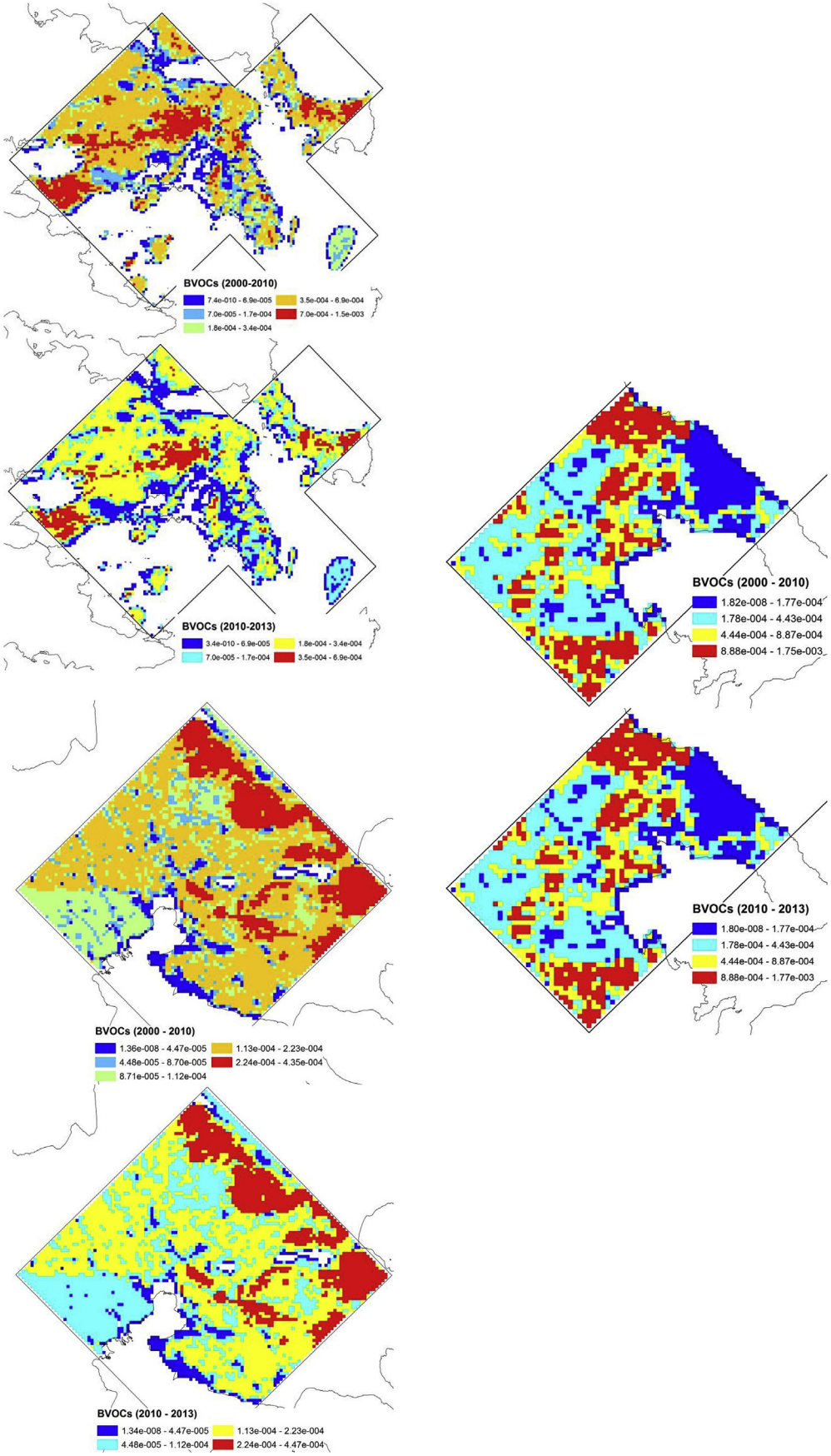


**Fig. 8.** Comparison between 2000-2010 and 2010–2013 of spatial weighting factors for BVOCs emissions in AMA, TMA and GVA. The values in the legend correspond to the 10%, 25%, 50% and 100% percentile of weighting factor values of the period 2010–2013.

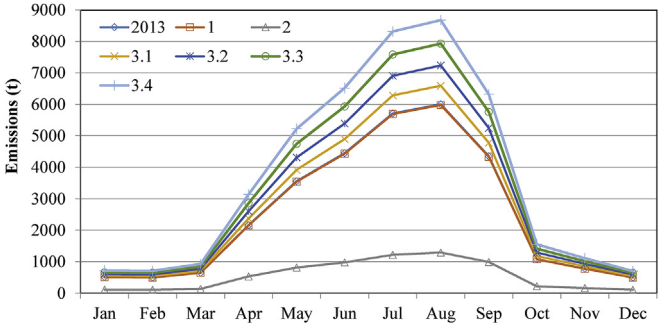


**Fig. 9.** Comparison of monthly variation of BVOCs emissions in AMA for different future scenarios. 2013: current emissions; 1: increase in artificial land; 2: all forests and semi-natural areas were burnt; 3.1–3.4: increase in temperature by 1–4 °C.

burning during winter.

### 3.2. Spatial distribution of natural emissions

Figs. 5–6 present the weighting factors which were used for the spatial disaggregation of natural PM emissions for the period 2010–2013. Based on the assumptions the spatial distribution coefficients remain unchanged throughout the period 2000–2013. In particular, no land cover changes are incorporated in the calculations and the values of meteorological conditions are averaged over each area of interest thus the spatial disaggregation coefficients are the same for every year for PM emissions and the same for $PM_{2.5}$ and $PM_{2.5\text{-}10}$. Inter-annual changes were found only in the cells including coastal areas which were considered insignificant (up to $5.6 \times 10^{-18}$).

The weighting factors for VOCs emissions are presented in Fig. 7 – 8. It is observed that natural PM emissions are scattered over arable land, areas with sclerophyllus vegetation and the sea. In particular, emissions of sea salt particles are equally distributed over the open sea whereas the variation of values at coastal cells corresponds to differences in the length and complexity of the shoreline. The spatial variation of windblown dust emissions is attributed to differences in the soil texture and land cover. With regards to land cover, the emission rates increase in the order of partly built-up areas to dense forest with higher values over agricultural land. The same trend applies also to the values of weighting factors with some discrepancy attributed to the aggregation of emissions in grid cells with variable landcover (see Fig. 1).

On the other hand, the weighting factors for BVOCs emissions spatial disaggregation vary seasonally and from year to year. In Fig. 7 the spatial weighting factors of BVOCs seasonal emissions are depicted. It is observed that BVOCs emissions in AMA are concentrated over the Northern part of the area, the Eastern part of the Attica peninsula, Evoia at the NE and the Gerania mountains at the W part of the domain where areas with significant natural vegetation occur (forests and semi-natural areas). In TMA BVOCs emissions are enhanced over the eastern part of the domain during both the warm and cold periods whereas in GVA emissions are mainly distributed over agricultural land.

BVOCs emissions scattered over the domains are mainly attributed to OVOCs which are emitted from every non-artificial surface. Changes in seasonal emissions weighting factors are attributed to the seasonal variation in emission factors and foliar biomass densities. For example, no emissions of BVOCs occur during the cold period over the deciduous forest in mountain Pilio in GVA.

In addition, in Fig. 8 the average spatial disaggregation coefficients of periods 2000–2010 and 2010–2013 are compared. As with the previous period, BVOCs emissions in AMA are concentrated over the Northern part of the area, the Eastern part of the Attica peninsula, Evoia at the NE and the Gerania mountains at the W part of the domain where areas with significant natural vegetation occur. However, the distribution of emission weighting factors in AMA is shifted to lower values compared to the previous period. For TMA and GVA the distributions of emission weighting factors remain relatively unchanged.

### 3.3. Emissions under different future scenarios

The changes in environmental conditions due to climate change are expected to affect the spatial and temporal distribution of emissions. In particular, the effects from changes in land cover and temperature, according to the three future scenarios examined (1: increase in artificial land by 2.7% with subsequent decrease in areas with natural, semi-natural and agricultural land cover - the meteorological conditions are same as in 2013; 2: all forests and semi-natural areas are burnt - the meteorological conditions are same as in 2013; 3: increase in temperature by 1–4 °C – land cover remains unchanged and same to 2013). The temporal distribution of emissions in AMA are presented in Fig. 9 (2013: current emissions; 1: increase in artificial land; 2: all forests and semi-natural areas were burnt; 3.1–3.4: increase in temperature by 1–4 °C). The same results with similar monthly variation apply also to TMA and GVA but with higher (y axis scale up to 16000 t) and lower (y axis scale up to 3500 t) values, respectively.

It is observed, that although the amount of emitted BVOCs varies significantly among the different scenarios, the monthly distribution of emissions remains relatively unchanged in all scenarios except for scenario 2 (applies to all areas). Specifically, for AMA the monthly contribution to annual BVOCs emissions was lowered during the cold period, in July and in August and it was enhanced during the rest months of the warm period (3%–12%). In TMA relatively less BVOCs were emitted during the period May–August (1%–11%) and in GVA from May to September (1%–11%). During the rest of the year the monthly contribution of BVOCs emissions to the annual was enhanced 2%–60% in TMA and 11%–74% in GVA. The above changes in TMA and GVA are attributed to the fact that more than half of the land (except for forest and semi-natural areas which are considered burnt) is covered by non-irrigated arable land that emits more than 50% of BVOCs during the warm period of the year. The projected increase of temperature (scenario 3) did not affect the monthly variation of BVOCs emissions however for an extended and warmer growing season enhanced emission rates are expected. On the other hand, the increased risk of forest fires and the contraction of forests (scenarios 1 and 2) can decrease the overall BVOCs production in the areas.

The decrease of precipitation, the contraction of forests, the increase of aridity and the reduction in extent and duration of snow cover can increase the windblown dust emissions. In particular, changes in the temporal distribution of soil dust emissions were examined by comparing emissions for the three scenarios (land use kept unchanged scenario 1: intermediate case – source inactive during and after rain and unlimited erosion potential, and 2: worst case - dry conditions and scenario 3: all forests and semi-natural areas are burnt and dry conditions) to 2013 emissions. The results are given in Fig. 10. Compared to dry conditions (scenario 2), monthly weighting factors of windblown dust are larger during the summer and lower during the winter when the effects from rain and snow cover are taken into account in the calculations (2013 emissions and scenario 1). The contraction of forests and semi-natural areas together with the prevalence of dry conditions results in approximately the same variation of monthly weighting factors with scenario 2. The warm/cold period emission ratios were for scenario 1: 1.13, 0.71 and 0.66 for AMA, TMA and GVA, respectively, while for scenarios 2 and 3 the corresponding values were 0.83, 0.59 and 0.52, respectively.

Finally, the increase of temperature and the contraction of forests can also affect the spatial distribution of BVOCs and windblown dust emissions. The spatial distribution of BVOCs in AMA and of windblown dust emissions in GVA under the different future scenarios are given in Fig. 11. It is observed that significant changes in land use, particularly with regards to forest and semi-natural areas, can result in different

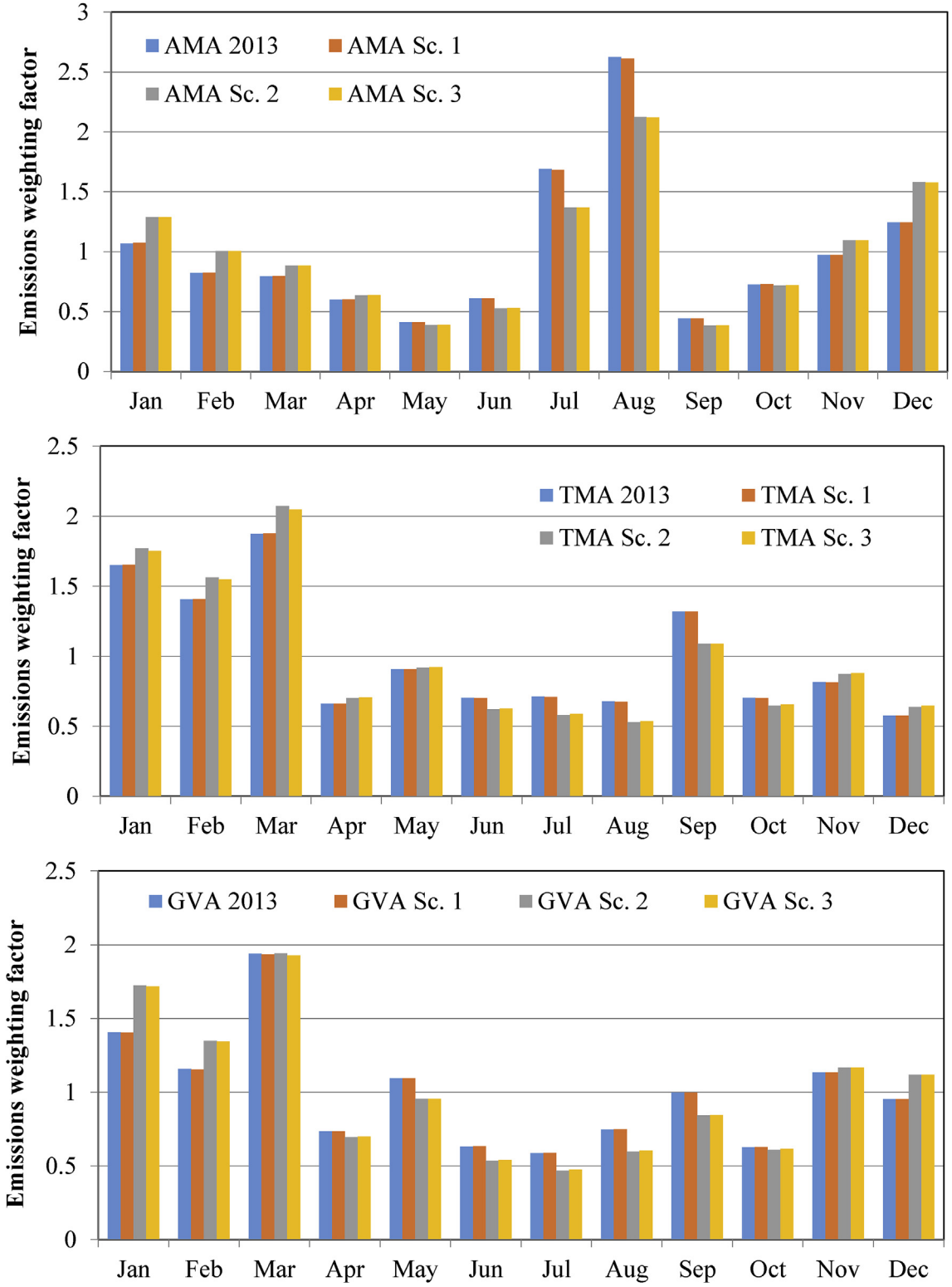


**Fig. 10.** Comparison of monthly variation of $PM_{10}$ windblown dust emissions for different future scenarios (variation around the mean). 2013: current emissions; 1: rain and unlimited erosion potential; 2: no rain; 3: no rain and all forests and semi-natural areas are burnt.

spatial distributions. On the other hand, small changes in temperature shift the distribution of weighting factors to higher values (the legend values correspond to the 1%, 10%, 25%, 33%, 50%, 75%, 90% and 100% percentile of weighting factor values for 2013; the same values correspond to the 1.1%, 11.4%, 28.6%, 37.7%, 57.1%, 85.7% and 100% for scenario 3.1). Additionally, the spatial distribution of windblown dust was found significantly altered only under scenario 3 i.e. dry conditions and burnt forests (the 2013 legend values correspond to the 1.6%, 15.9%, 39.6%, 52.2% and 79.10% of WF distribution for scenario 3).

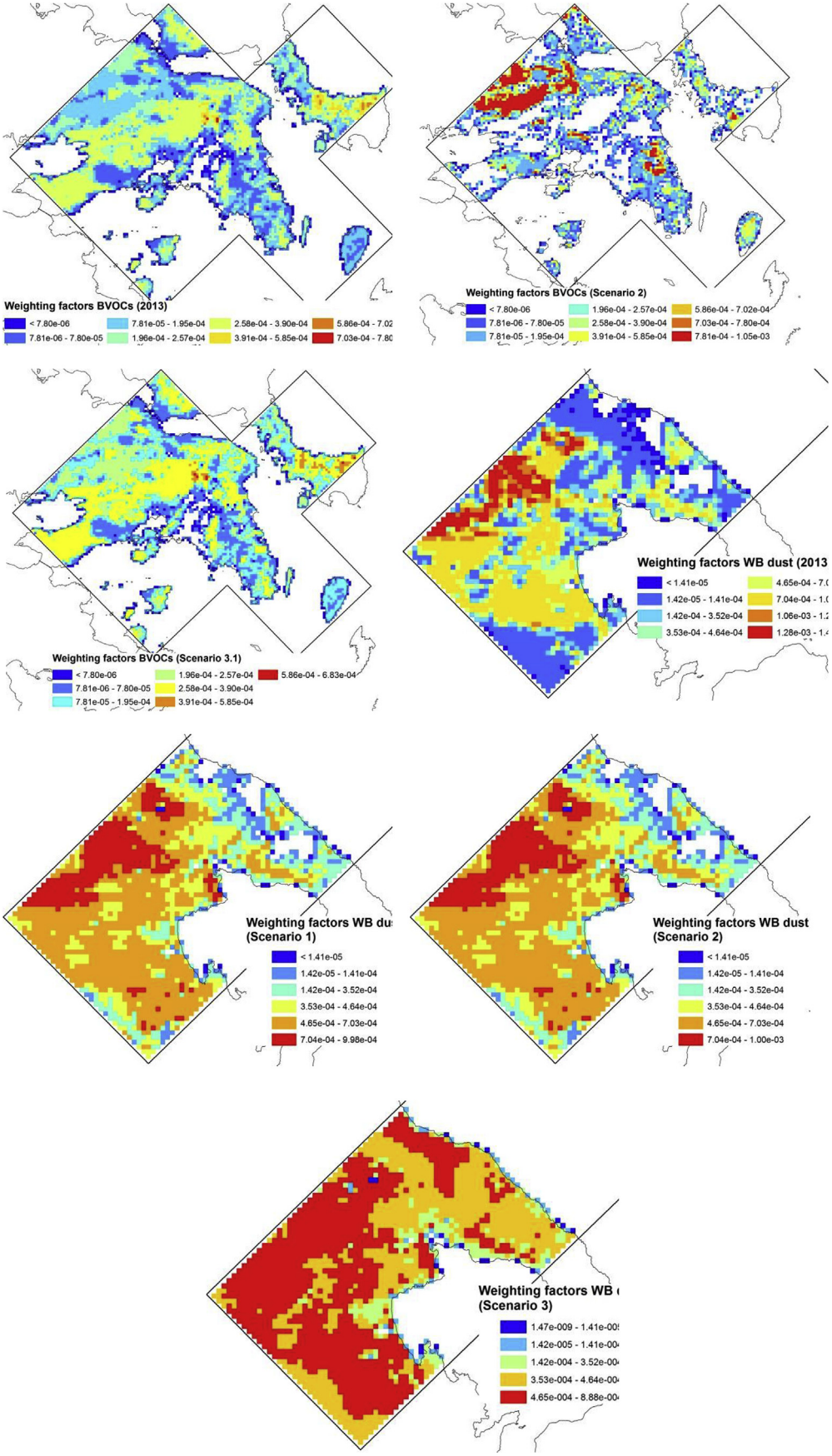


**Fig. 11.** Comparison of spatial weighting factors for BVOCs emissions in AMA and $PM_{10}$ windblown dust emissions in GVA for different future scenarios. Scenarios for BVOCs: 2013 - current emissions, 2 - all forests and semi-natural areas are burnt and 3 - 1 °C increase in temperature. Scenarios for WB dust emissions: 2013 - current emissions, 1 - rain and unlimited erosion potential, 2 - no rain and 3 - no rain and all forests and semi-natural areas are burnt. The legend values correspond to the 1%, 10%, 25%, 33%, 50%, 75%, 90% and 100% percentile of WF values for 2013.

## 4. Conclusions

Monthly emissions of primary PM from natural sources in three urban areas in Greece (metropolitan areas of Athens, Thessaloniki and Volos) were calculated during the period 2010–2013 and for projected future climatic scenarios.

The current study showed first that the BVOCs emissions during the period 2010–2013 in the three urban areas in Greece were enhanced compared to 2000–2010 whereas natural PM emissions have lowered. These changes reflect mainly the variability of the meteorological conditions.

In addition, specific climatic change scenarios were introduced based on future changes in land cover and environmental conditions. The projected changes in temperature and precipitation did not affect considerably the temporal and spatial distribution of natural emissions while considerable emission changes were observed for significant land use modifications together with the prevalence of dry conditions.

## References


Aleksandropoulou, V., Lazaridis, M., 2004. Spatial distribution of gaseous and particulate matter emissions in Greece. Water Air Soil Pollut. 153, 15–34.

Aleksandropoulou, V., Torseth, K., Lazaridis, M., 2011. Atmospheric emission inventory for natural and anthropogenic sources and spatial emission mapping for the greater Athens area. Water Air Soil Pollut. 219, 507–526.

Aleksandropoulou, V., Torseth, K., Lazaridis, M., 2013. The effect of forest fires in emissions of Biogenic Volatile Organic Compounds and windblown dust over urban areas. Air Qual. Atmos. Health 6, 277–294.

Aleksandropoulou, V., Torseth, K., Lazaridis, M., 2015. The contribution from natural sources to PM emissions over the metropolitan areas of Athens and Thessaloniki. Aerosol Air Qual. Res. 15, 1300–1312.

Ashworth, K., Wild, O., Hewitt, C.N., 2010. Sensitivity of isoprene emissions estimated using MEGAN to the time resolution of input climate data. Atmos. Chem. Phys. 10, 1193–1201.

Athanasopoulou, E., Tombrou, M., Russell, A.G., Karanasiou, A., Eleftheriadis, K., Dandou, A., 2010. Implementation of road and soil dust emission parameterizations in the aerosol model CAMx: applications over the greater Athens urban area affected by natural sources. J. Geophys. Res. 115, D17301.

De Leeuw, F., 2002. A set of emission indicators for long-range transboundary air pollution. Environ. Sci. Pol. 5 (2), 135–145.

De Leeuw, G., Neele, F.P., Hill, M., Smith, M.H., Vignali, E., 2000. Production of sea spray aerosol in the surf zone. J. Geophys. Res. Atmos. 105, 29397–29409.

EEA, 2012. Report No 12/2012. Climate Change, Impacts and Vulnerability in Europe 2012. . http://www.eea.europa.eu/publications/climate-impacts-and-vulnerability-2012.

EEA, 2013. Analysis of Changes in European Land Cover from 2000 to 2006. http://www.eea.europa.eu/data-and-maps/figures/land-cover-2006-and-changes-1.

EEA CLC2000, 2009. Corine Land Cover 2000 (CLC2000) 100 M - Version 12/2009(2009). http://www.eea.europa.eu/data-and-maps/data/corine-land-cover-2000-clc2000-100-m-version-12-2009/.

FOODSEC Meteodata Distribution Page. http://mars.jrc.ec.europa.eu/mars/About-us/FOODSEC/Data-Distribution.

Grini, A., Myhre, G., Sundet, J., Isaksen, I., 2002. J. Clim. 15 (13), 1717–1730.

Hodnebrog, O., Solberg, S., Stordal, F., Svendby, T.M., Simpson, D., Gauss, M., Hilboll, A., Pfister, G.G., Turquety, S., Richter, A., Burrows, J.P., van der Gon, H.A.C.D., 2012. Impact of forest fires, biogenic emissions and high temperatures on the elevated Eastern Mediterranean ozone levels during the hot summer of 2007. Atmos. Chem. Phys. 12, 8727–8750.

Kalnay, et al., 1996. The NCEP/NCAR 40-year reanalysis project. Bull. Am. Meteorol. Soc. 77, 437–470.

Katsouyanni, K., Touloumi, G., Samoli, E., Gryparis, A., Le Tatre, A., Monopolis, Y., Rossi, G., Zmirou, D., Ballester, F., Boumghar, A., Anderson, H., Wojtyniak, B., Paldy, A., Barunstein, R., Pekkanen, J., Schnidler, C., Schwartz, J., 2001. Confounding effect modification in the short-term effects of ambient particles on total mortality: results from 29 European cities within the APHEA 2 project. Epidemiology 12, 521–531.

Korcz, M., Fudala, J., Klis, C., 2009. Estimation of wind blown dust emissions in Europe and its vicinity. Atmos. Environ. 43 (7), 1410–1420.

Oderbolz, D.C., Aksoyoglu, S., Keller, J., Barmpadimos, I., Steinbrecher, R., Skjoth, C.A., Plass-Duelmer, C., Prevot, A.S.H., 2013. A comprehensive emission inventory of biogenic volatile organic compounds in Europe: improved seasonality and land-cover. Atmos. Chem. Phys. 13, 1689–1712.

Pope, C.A., Burnett, R.T., Thun, M.J., Calle, E.E., Krewski, D., Ito, K., Thurston, G.D., 2002. Lung Cancer, Cardio-pulmonary mortality and Long-term exposure to fine particulate air pollution. J. Am. Med. Assoc. 287 (9), 1132–1141.

Pope, C.A., Thun, M.J., Namboodiri, M.M., Dockery, D.W., Evans, J.S., Speizer, F.E., Heath Jr., D.W., 1995. Particulate air pollution as a predictor of mortality in a prospective study of U. S. adults. Am. J. Respir. Crit. Care Med. 151, 669–674.

Pugh, T.A.M., Ashworth, K., Wild, O., Hewitt, C.N., 2013. Effects of the spatial resolution of climate data on estimates of biogenic isoprene emissions. Atmos. Environ. 70, 1–6.

Symeonidis, P., Poupkou, A., Gkantou, A., Melas, D., Yay, D., Pouspourika, E., Balis, D., 2008. Development of a computational system for estimating biogenic NMVOCs emissions based on GIS technology. Atmos. Environ. 42 (8), 1777–1789.

Winiwarter, W., Kuhlbusch, T.A.J., Viana, M., Hitzenberger, R., 2009. Quality considerations of European PM emission inventories. Atmos. Environ. 43 (25), 3819–3828.

Zhang, K.M., Knipping, E.M., Wexler, A.S., Bhave, P.V., Tonnesen, G.S., 2005. Size distribution of sea-salt emissions as a function of relative humidity. Atmos. Environ. 39, 3373–3379.